Article

FL* Approach to the Coexistence of Fermi Arcs with Metal–Insulator Crossover in Strongly Underdoped Cuprates

Pieralberto Marchetti

Dipartimento di Fisica e Astronomia, Università di Padova, INFN, I-35131 Padova, Italy;
pieralberto.marchetti@unipd.it

Abstract: We propose that one can explain the coexistence in the same range of doping and temperature of gapless Fermi arcs with the metal–insulator crossover of in-plane resistivity in strongly underdoped cuprates in terms of the FL* fractionalized Fermi liquid nature of these systems, and that such coexistence is not due simply to disorder effects in the resistivity. The particle excitations of this FL* system derived from variants of the *t-J* model are the gapless holon carrying charge with small Fermi momentum proportional to the doping, the gapful spinon carrying spin 1/2, and an emergent gauge field coupling them and the hole as a spinon–holon bound state, or more precisely resonance, due to gauge binding, with a Fermi surface respecting the topological Luttinger theorem. In our proposal, Fermi arcs are determined by the hole resonance, whereas the metal–insulator crossover is dominated by spinon–spinon (with subleading holon–holon) gauge interactions, and this dichotomy is able to explain their coexistence.

Keywords: cuprates; fractionalized Fermi liquid; *t-J* model

1. Introduction

In the strong-underdoping low-temperature region of the phase diagram of the cuprates, the existence of gapless Fermi arcs has been proved by ARPES experiments (see, e.g., [1] and references therein). According to the Fermi liquid paradigm then one would expect a metallic resistivity with a temperature dependence T^α, with α at least greater than 1. In the same region of the phase diagram, however, the experiments show that the in-plane resistivity has a minimum at finite temperature, i.e., a metal–insulator crossover (see, e.g., [2]). Furthermore, a suitably normalized resistivity exhibits a universal behavior [3] that seems hardly compatible with an explanation of that crossover in terms of disorder-induced localization.

We propose that one can explain the coexistence of the two phenomena in terms of the FL* fractionalized Fermi liquid concept, introduced in [4,5], within an approach to the low-energy physics of the cuprates in terms of the *t-t'-J* model.

There have been several proposals of an FL* nature of the above-quoted region of the phase diagram of the cuprates, named the "pseudogap phase" ([6,7] and references therein), but to our knowledge not a careful discussion of the consistency between Fermi arcs and the metal–insulator crossover (MIC).

An FL* is an exotic fractionalized Fermi liquid which has hole-like (in the case relevant for the cuprates) excitations near a Fermi surface satisfying a generalization of the Luttinger theorem, together with fractionalized excitations emerging from a topological order, in particular charged spinless holons (*h*) and neutral spin 1/2 spinons (*s*), interacting via a so-called slave-particle gauge field (*a*). The hole is a bound state or a resonance arising from holon–spinon binding induced by the gauge attraction.

The present paper is part of a project aimed at analyzing the consequences of the proposed FL* nature of the cuprates. The general idea underlying this project is that one can explain the Fermi liquid (FL) versus non-Fermi liquid (NFL) dichotomies encountered in the cuprates, in the present case the FL nature of Fermi arcs and the NFL nature of the

MIC, in the following way: If some physical response is dominated by the hole excitations (holon–spinon interaction), then its behavior is similar to that of a Fermi liquid; if instead it is dominated by spinon–spinon (and possibly also holon–holon) interaction, then it clearly has characteristics of a non-Fermi liquid.

It is known of course that the t-t'-J model is not sufficient to explain some phenomena exhibited by the cuprates, such as charge density waves (see, e.g., [8]), but apparently for the issue of the present paper, at strong underdoping at least, these phenomena are qualitatively irrelevant [9]. More generally, although clearly such a simple model cannot reproduce real experimental data, we show that even with an approximate treatment many of their doping and temperature dependencies can be indeed qualitatively understood. Furthermore, with the introduction of experimentally derived but doping- and temperature-independent scales also a semi-quantitative agreement is obtained in many cases (e.g., for the universal curves of normalized resistivity, discussed also here in Section 4, and for the normalized superfluid density in the underdoping region [10]).

2. General Outline of the Approach

In the description of the low-energy physics of the cuprates in terms of a two-dimensional (2D) t-t'-J model, the sites of the model correspond to the Cu sites of a CuO plane in the cuprates and the empty sites of the model to the Zhang–Rice singlets. The Hamiltonian is given by

$$H = P^G[\sum_{<i,j>n.n.} -tc_{i\alpha}^* c_{j\alpha} + h.c. + J\vec{S}_i \cdot \vec{S}_j + \sum_{<i,j>n.n.n.} t' c_{i\alpha}^* c_{j\alpha}]P^G, \tag{1}$$

where $< i, j >$ denotes a link between lattice sites i and j, $(n)n.n.$ denotes the (next-)nearest neighbor sites, and α is the spin index, which is assumed to be summed up also in the following if repeated. The Gutzwiller projection is denoted by P^G and it implements the no-double-occupation constraint, describing the Mott physics of the system. It can be tackled with a spin-charge decomposition [11,12] of the hole field: $c_\alpha = hs_\alpha^*$, where the holon h is a spinless fermion, thus implementing the no double occupation by the Pauli principle, and the spinon s is a boson, satisfying in each site the constraint $s_\alpha^* s_\alpha = 1$ [13]. This decomposition generates an unphysical degree of freedom, since one can multiply at each site s and h by arbitrary opposite phase factors leaving c unchanged. The corresponding local $U(1)$ gauge invariance is implemented by introducing a slave-particle gauge field a_μ that in turn produces an attraction between holon and spinon. To show this effect of the emerging gauge field beyond perturbation theory we apply in [14], as a rough approximation, a kind of eikonal resummation (some details are sketched in Appendix A).

However, a comparison with the corresponding one-dimensional (1D) model [15,16] suggests modifying the statistics of spinons and holons at the lattice level, turning them into semions, i.e., under equal-time-oriented exchanges their fields acquire a phase $\pm\pi/2$ (see, e.g., [17]). These phase factors are opposite for spinons and holons, so that c retains its fermionic nature. This modified statistics is crucial for our discussion (as it was in one dimension), so let us give some details.

The change in statistics is implemented in the Lagrangian formalism by coupling the holon to a $U(1)$ gauge field B_μ, related to the charge, with a Chern–Simons action with coefficient $-1/2$, and coupling the spinon to an SU(2) gauge field V_μ, related to the spin, with Chern–Simons action with coefficient $1/2$ [13,18]. This procedure corresponds to dressing the holon with a $-1/2$ charge flux and the spinon with a $1/2$ spin flux. Due to the topological properties of Chern–Simons theory, if no approximations are made, the result is an exact rewriting of the original model. However, if suitable approximations are introduced, this rewriting provides a treatment of the model that with dimensional reduction was successful in deriving the correct large-scale behavior of the model in 1D [15]. Therefore, we suggested that this provides a good approach also for the 2D model, relevant for the low-energy physics of the cuprates. The parameter region corresponding to what we call in this paper the pseudogap (PG) "phase" of the cuprates has an upper boundary

in the (in-plane) doping (δ)-temperature (T) phase diagram identified with the inflection point of in-plane resistivity [2]. Therefore, the PG "phase" appears at low δ and T.

In PG, the holon dressing by the charge gauge field B_μ induces a "uniform" (staggered) charge-flux $\pm \pi$ per plaquette [13]. Through the Hofstadter mechanism [19] it converts the spinless fermionic holons h into lattice Dirac fermions, with dispersion defined in the magnetic Brillouin zone (MBZ). More precisely, the results of [20] prove that for elementary circuits, triangles and squares, in the t-t' model the optimal flux at half-filling is $\pi/2$ for triangles and π for squares. Therefore, we assume at sufficiently small doping and temperature the following structure for the "uniform" component of B, denoted as in [21] by $B_\mu^m, \mu = 1, 2$: Let i denote a site in the even Néel sublattice and $i \pm \hat{\alpha}, \alpha = 1, 2$ its nearest-neighbor sites in the 1 and 2 directions, respectively, and $i + \hat{\beta}, \beta = \pm 1 \pm 2$ its next-nearest-neighbor sites. Then,

$$\int_{<i,i\pm\hat{\alpha}>} B_\mu^m dx^\mu = (-1)^\alpha (\pm 1) \frac{\pi}{4}, \quad \int_{<i,i\pm\hat{\beta}>} B_\mu^m dx^\mu = \pi \tag{2}$$

The fluctuations of B_μ around its "uniform" component turn the holons into semions. Since semionic spinless excitations have the same Fermi surface (FS) of spin $1/2$ fermions [22,23], the above π flux converts the fermionic holon with tight-binding dispersion

$$\omega_h \sim 2t[(\cos k_x + \cos k_y) - \delta] + 4t' \cos k_x \cos k_y \tag{3}$$

into a pair of lattice "Dirac fields", ψ_a, with pseudospin index a related to the two Néel sublattices and with dispersion

$$\omega_h \sim 2t[\sqrt{\cos^2 k_x + \cos^2 k_y} - \delta] - 4t' \cos k_x \cos k_y \tag{4}$$

restricted to the magnetic Brillouin zone. This produces small holon Fermi surfaces near $(\pm\pi/2, \pm\pi/2)$ with Fermi momenta k_h^F of $O(\delta)$ in the MBZ, if identified with the union of two square regions, denoted as R(ight) and L(eft) centered at $Q_R = (\pi/2, \pi/2)$ and $Q_L = (-\pi/2, \pi/2)$, respectively. In the hole spinon–holon resonance, the Dirac structure of such holons induces [14] a momentum-dependent factor in the wave-function renormalization constant,

$$Z(\vec{k}) = \frac{1}{2}[1 - \frac{\cos k_x + \cos k_y}{\sqrt{2}\sqrt{\cos k_x^2 + \cos k_y^2}}] \tag{5}$$

which reduces the spectral weight in the outer boundary of the MBZ, one key ingredient for a phenomenology of Fermi arcs at strong underdoping.

Let us turn to the gauge field associated with spin. The leading $SU(2)$ component of the V_μ field is along the magnetization axis of the undoped model. It introduces an interaction with the spinons, whose dynamics without V_μ at large scales is described by a CP1 model, leading to an additional term,

$$J'(V^\mu)^2 s_\alpha^* s_\alpha, \tag{6}$$

where, as a result of a mean-field approximation, $J' \approx J(1 - 2\delta)$. Neglecting a staggered "uniform" term with mean zero, the field V_μ describes quantum vortices centered on the positions of lattice holons, with opposite chirality for the two Néel sublattices, so that we call them "antiferromagnetic (AF) spin" vortices. In a quenched treatment of such vortices, we derive the mean-field expectation value $< (V^\mu)^2 > = m_s^2$, with $m_s^2 \approx 0.5\delta|\log \delta|$. This opens a mass gap $J'm_s$ for the spinon that turns out to be consistent with the AF correlation length at small δ extracted from the neutron experiments [24]. Therefore, the originally AF gapless spinons of the undoped Heisenberg model propagating in the gas of slowly moving AF spin vortices acquire a finite gap, giving rise to a short-range AF order.

This spinon gap is crucial because the spinon contribution to the slave-particle gauge action is then of Maxwell type, hence subleading with respect to the contribution of gapless holons. The holon contribution is characterized by the Reizer singularity in the dominant transverse component, killing the logarithmic confinement induced by the spinon contribution. Without the spinon gap the CP1 model would be in the broken symmetry "Higgs" phase and the spinon contribution to the gauge action would be gapped by the Anderson–Higgs mechanism, thus becoming the dominant one. As shown below, the Reizer singularity of the slave-particle gauge field is a key factor for the discussion of resistivity and Fermi arcs. In particular, the gauge interaction turns the spinon mass m_s into a "complex temperature- and frequency-dependent mass" $M_s(T, \omega) = \sqrt{m_s^2 + ic \frac{((\pi T)^2 + \omega^2)^{1/2}}{\chi}}$, where c is a real constant of $O(1)$ and χ the holon diamagnetic susceptibility, proportional to $1/\delta$. Furthermore, the spinon gap modifies the chemical potential of the holes with respect to that of the holons so that the Fermi momentum is of $O(\delta^{1/2})$. The binding with the spinons produces a hole FS given by four small components centered at $(\pm\pi/2, \pm\pi/2)$. The π-flux introduces a topological order and the relevant version of the topological Luttinger theorem with the relation "fraction of the area of the BZ enclosed by the hole FS" = $\delta/2$ is satisfied. This is possible due to the modification of the holon chemical potential and actually, somewhat surprisingly, even a simple doping-independent combination of the holon Fermi momenta and the spinon momenta corresponding to the spinon gap produces an area of the hole FS quite well compatible with that of the Luttinger theorem, for all the dopings in the physical range.

The above results show that the system behaves like an FL* liquid. Furthermore, with the choice of B^m made above, the FS of the hole near the diagonals of the BZ, where most of the spectral weight is concentrated, almost overlaps with the large tight-binding FS; see Figure 1. This is necessary for consistency with the ARPES data, although admittedly, the overlap obtained is not enough.
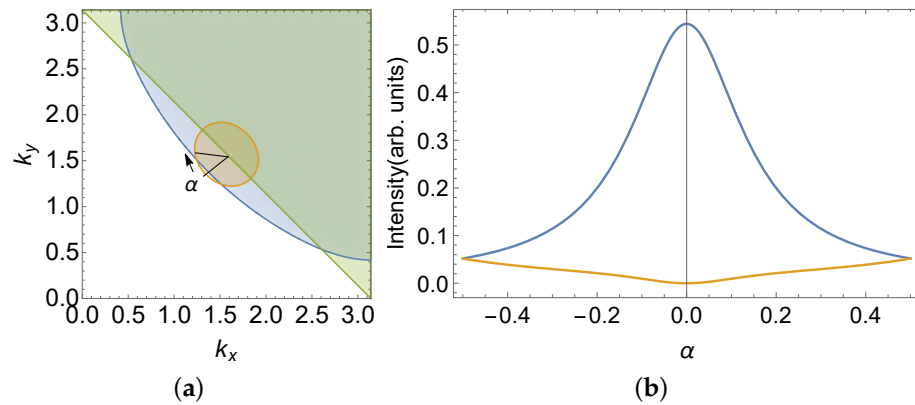

(a)   (b)

Figure 1. (a) Exterior of the MBZ (green), interior of the tight-binding FS for the hole (blue), and interior of the small FS in PG derived as discussed in the text (orange) in the first quadrant of the BZ for $t'/t = 0.25$ and $\delta = 0.07$. The angle along the small FS in PG is denoted by α as in the text. (b) Intensity of the symmetrized spectral weight of the hole along the small FS in PG shown in (a) at $T = 20$ K. The intensity inside the MBZ is in blue, that outside in yellow. α is measured in units of π and the origin is shifted by -1 outside of the MBZ.

The last ingredient crucial in our discussion is a long-range attraction between the AF spin vortices centered on holons in two different Néel sublattices. If we treat in mean-field the spinons ($< s_\alpha^* s_\alpha >$) in Equation (6) we see that the interaction mediated by AF spin vortices on holons is of a 2D Coulomb type. According to the behavior of planar Coulomb systems below a crossover temperature $T_{ph} \sim J'/2\pi$, a finite density of incoherent holon pairs appears. As previously remarked, the low-energy holon modes in PG have two small FSs in the MBZ; the 2D Coulomb interaction acts on these modes coupling opposite sites

of each FS with an attractive potential whose range is given by the screening length of the Coulomb gas. If such an attraction is treated in the BCS approximation it provides a p-wave pairing on the two FSs that, glued in the entire BZ for the hole resonance, produce a d-wave-order parameter, as first suggested in a different approach in [25]. However, such holon pairs do not condense because the fluctuations of the phase of the pairing field are actually too strong [26], so that the slave-particle gauge symmetry broken by the BCS approximation is restored.

3. FL* Approach to Fermi Arcs

Let us summarize in precise terms the output of the above considerations on the self-energy of the hole resonance (see Appendix A for some details). The binding induced by the gauge fluctuations dominated by the Reizer singularity computed with the above-cited eikonal approximation produces an imaginary part of the self-energy of the form

$$\Gamma(\omega, T) = \Im\Sigma_g(\omega, T)] = -\Im[J(1 - 2\delta)\sqrt{m_s^2 + ic\frac{((\pi T)^2 + \omega^2)^{1/2}}{\chi}} =$$

$$-J(1 - 2\delta)(m_s^4 + (c^2\frac{(\pi T)^2 + \omega^2}{\chi^2}))^{1/4}\sin[\frac{1}{2}\arctan(c\frac{((\pi T)^2 + \omega^2)^{1/2}}{m_s^2\chi})]. \tag{7}$$

Notice that $\Im\Sigma_g(\omega, 0)$ is linear in $|\omega|$ for sufficiently small frequencies; therefore, the hole-resonances in PG behave like a marginal Fermi liquid [27]. Indeed, such behavior was found first in optimally [28] and then also in underdoped [29] cuprates.

The contribution to the real part of the self-energy, $\Re\Sigma_g(\omega, T)$, corresponding to Equation (7), is estimated using a Kramers–Kroenig procedure, with a UV cutoff at the charge-transfer gap $\approx 4J$, as suggested by experimental data.

An additional T^2 term can arise due to standard Landau hole–hole interactions.

Let us turn to the effect of the attraction induced by the AF spin vortices.

In our approximation, we keep constant (up to its d-structure) the modulus of the holon-pairing parameter $\Delta_h(\vec{k})$, obtained as the solution of a BCS-like equation [26], near the Fermi surface. However, since the charge pairs are not condensed its phase is strongly fluctuating. Therefore, the field describing these phase fluctuations, $\exp i\phi$, has a doping- and temperature-dependent gap, denoted by m_ϕ, decreasing with T and modifying the standard BCS form of the self-energy near the hole Fermi surface. For $m_\phi(T, \delta)$ we adopt a form suggested in [30]:

$$m_\phi(T, \delta) \approx T_{ph}(\delta)e^{-\sqrt{\frac{T_{ph}(\delta) - T}{T - T_{pc}(\delta)}}}, \tag{8}$$

where $T_{pc}(\delta)$ is (an estimate of) the temperature of condensation of holon pairs, which, however, never occur in the parameter range considered (in [31] it was set to 0). A reasonable approximation for the contribution to the self-energy turns out to be [32]

$$\Sigma_v(\omega, \vec{k}, T) \approx$$

$$\frac{|\Delta_h(\vec{k}, T)|^2}{\omega - \omega_h(\vec{k}, \omega, T) + i\Gamma(\omega, T)}[1 - \frac{m_\phi(T)}{\sqrt{-(\omega + i\Gamma(\omega, T))^2 + \omega_h(\vec{k}, \omega, T)^2 + m_\phi(T)^2}}] \tag{9}$$

where ω_h is the hole dispersion modified by $\Re\Sigma_g(\omega, T)$ (subleading modifications are not taken into account in [32]) and Γ is the scattering rate of the hole without charge pairing. To understand its implications, let us consider its behavior in two regions of energy: For $\omega \ll m_\phi$, expanding the self-energy up to the second order in terms of ω/m_ϕ we obtain

$$\Sigma_v(\omega, \vec{k}, T) \approx \frac{|\Delta_h(\vec{k}, T)|^2}{2m_\phi(T)}(\omega - \omega_h(\vec{k}, \omega, T) + i\Gamma(\omega, T))) \tag{10}$$

We see that for low frequencies the effect of the holon pairing appears through a contribution to the wave-function renormalization constant, not modifying the marginal FL nature but with a strong dependence on the direction of $\vec{k}$ that, together with the Dirac structure, heavily suppresses the spectral weight along the hole FS as we move towards the MBZ boundary from a point in the diagonal inside the MBZ; see Figure 1. The "shadow band" outside of the MBZ may then be invisible because it disappears in the background incoherent continuum.

For $\omega >> m_\phi$, we expand the self-energy in powers of m_ϕ/ω and we obtain

$$\Sigma_v(\omega, \vec{k}, T) \approx \frac{|\Delta_h(\vec{k}, T)|^2}{\omega - \omega_h(\vec{k}, \omega, T) + i\Gamma(\omega, T)} \tag{11}$$

which is the self-energy of a d-wave superconductor. The spectral weight is symmetric in frequencies and non-vanishing on the FS, but it exhibits two symmetric superconducting (SC)-like peaks, approximately at $\pm\sqrt{|\Delta_h(\vec{k}, T)|^2 + m_\phi(T)^2}$. It turns out that for $|\Delta_h(\vec{k}, T)| \gtrsim m_\phi(T)^2/\Gamma(\omega, T)$, such SC-like peaks cover the FL peak in the spectral weight. Due to the k-dependence of $\Delta_h(\vec{k}, T)$ near the nodal region, the spectral weight behaves in an FL-like manner, with an effective FS; while as we move towards the antinodal directions, most of the spectral weight is concentrated on the SC-like modes. Then, although there is an FS, it has negligible effects. We identify the Fermi arcs as the region of the FS where the FL peak is the dominant one; see Figure 2. As a consequence of the temperature dependence of m_ϕ, the Fermi arcs shrink as we lower T (see Figure 3), in agreement with experiments [33,34].
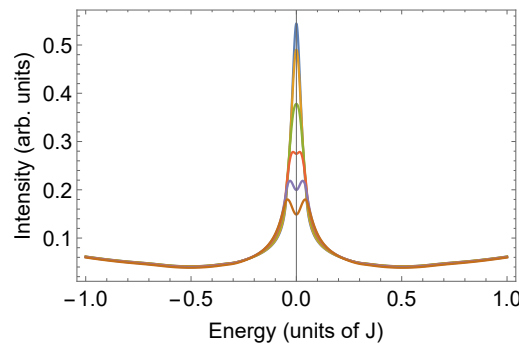

Figure 2. Symmetrized spectral weight of the hole along the small FS in Figure 1 at $T = 20$ K for $\alpha = n \cdot 0.05\pi, n = 0$ (top line, blue), 2, …, 5 (bottom line, brown). The increase at high energy is due to an approximate estimate of the incoherent holon–spinon contribution discussed in the text.
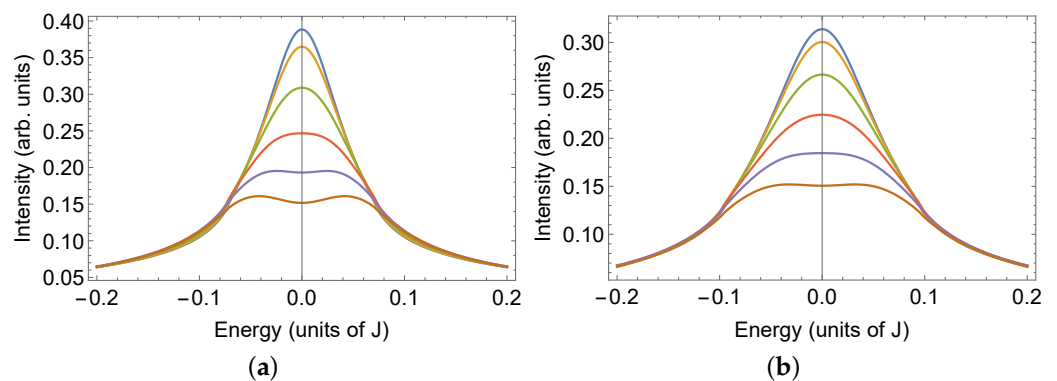

Figure 3. (a) Detail of the low-energy symmetrized spectral weight of the hole along the small FS as in Figure 2 at $T = 30$ K and (b) at $T = 40$ K.

The above computations clearly show that the effect of the gauge fluctuations on the hole resonance in PG is to produce an isotropic marginal FL behavior at low energy. Instead, the effect of the vortex attraction is an anisotropic d-wave-like contribution on the Fermi arcs and an effective gap outside of them. This suppression of the spectral weight away from the diagonals of the BZ induced by AF vortices, combined with the suppression of the wave-function renormalization constant due to the Dirac structure (see Equation (5)), produces a strong suppression of the spectral weight outside of the MBZ. Perhaps in this region the corresponding ARPES signal disappears in the thermal continuum background so that the Fermi arc might appear as consistent with the tight-binding Fermi surface. Small deviations near the boundary of the MBZ are however expected, as in [35].

Actually [32], above the continuum background, in addition to the coherent hole peak there is an additional contribution to the hole spectral weight of the incoherent part describing the high-energy momentum contribution of the unbinded spinon holon system; see Figure 2. Its leading contribution on the FS of the hole at energy ω can be approximately estimated as $DOS_h(\omega - m_s)/(2m_s)$ if $\omega > m_s$, where we denote by DOS_h the density of states of the holon. Due to the linear dispersion of the holon in the PG, DOS_h is approximately linear in its argument. Hence, the incoherent component of the hole gives a contribution to the spectral weight at positive ω that grows approximately linearly in ω starting from m_s. This additional linear contribution agrees with the ARPES data in strongly underdoped cuprates (see, e.g., [36]).

4. FL* Approach to Metal–Insulator Crossover

In strongly underdoped cuprates, or more precisely in PG, the in-plane resistivity ρ exhibits a quite peculiar behavior: it increases more than linearly at intermediate temperatures, with a T^2 behavior in the same range, but at lower temperatures, unless it drops to zero at the critical temperature, it acquires an insulating behavior. For sufficiently underdoped samples, therefore, one can identify a minimum in resistivity at a given temperature, denoted by T_{MIC}, marking a metal–insulator crossover. As previously mentioned, at higher temperatures, above the T^2 behavior, there is an inflection point in the resistivity as a function of temperature that is frequently used in defining the lower pseudogap temperature T^*.

Often, the MIC is attributed to disorder-induced localization. However, this interpretation is at odds at least with the following facts: (i) The role of true disorder has been analyzed carefully in [37] and although it can induce a MIC, the slope of the metallic behavior in this case is independent of the degree of disorder, whereas such a slope in the standard situation depends on the doping concentration. Perhaps instead the disorder is responsible for the logarithmic behavior found below the MIC. (ii) If the resistivity is suitably normalized it exhibits a universal behavior [3], being both doping- and even essentially material-independent in terms of T/T^*. Due to this universality, one can see a relation between T_{MIC} and T^*; the last one has been shown to be independent of disorder [37], reinforcing the idea that the MIC is not caused by disorder.

If the MIC is intrinsic it would be incompatible with the FL nature of Fermi arcs. In fact, following the analysis of the previous section, on the basis of the existence of gapless Fermi arcs with marginal FL behavior, using the Drude formula one would expect the in-plane resistivity to exhibit a metallic, linear-in-T behavior in PG. However, in an FL* theory, since spinons and holons interact via the slave-particle gauge field, one should see whether the contribution of the hole–hole interaction, due to spinon–holon coupling, is predominant, or is it the contribution due to spinon–spinon and holon–holon interactions. It turns out that the second alternative gives the leading effect for in-plane resistivity. To estimate the spinon–spinon interaction we employ the Kubo formula for the spinon current and adopt the above-mentioned eikonal approximation. For the holons, since the minimal coupling to Chern–Simons gauge fields does not change local gauge-invariant quantities, we can use the Drude formula. Then, the spinon and holon contributions are summed up following the Ioffe–Larkin rule [38], i.e., the resistivity of the two subsystems are added: $\rho = \rho_s + \rho_h$. Due to the slave-particle gauge interaction, the holon contribution is given by the standard

expression [39,40] $\rho_h \sim (T/\epsilon_h)^{4/3}$, where $\epsilon_h = t\delta$ is the holon Fermi energy. As discussed in detail in [14], the Reizer singularity of the slave-particle gauge field modifies the spinon current correlator, giving rise to a contribution to the in-plane resistivity given by

$$\rho_s \approx \sqrt{\frac{m_s}{\delta}} \frac{\left[1 + \left(\frac{1}{m_s\lambda_T}\right)^4\right]^{\frac{1}{8}}}{\sin\left[\frac{1}{4}\arctan\left(\frac{1}{m_s\lambda_T}\right)^2\right]} \tag{12}$$

where $\lambda_T = (\chi/\pi Tc)^{\frac{1}{2}} \sim (\delta T)^{-\frac{1}{2}}$ is a kind of "thermal de Broglie wavelength". Notice that the constant c here is the same used in the discussion of the Fermi arc and $T^* \approx 2\chi m_s^2$. For $T \gtrsim 100$ K up to almost T^* one finds a metallic behavior, $\sim T^2$, but in the limit $\lambda_T \geq m_s^{-1}$ the ρ_s exhibits an insulating behavior, $\sim \frac{1}{T}$ for low T. Such a spinon contribution is dominating with respect to the metallic holon contribution, so that the resistivity emerging from the Ioffe–Larkin rule at low T is still insulating and the overall behavior is semi-quantitatively consistent with the experimental data (except at lower T where, as remarked above, perhaps standard localization occurs); see Figure 4. This metal–insulator crossover is determined by the competition between the insulating behavior due to the AF correlation length m_s^{-1} and dissipation behavior due to the thermal de Broglie wave length λ_T. In particular, in the limit $\lambda_T \geq m_s^{-1}$ one finds a kind of localization effect on the spinon contribution generated by the short-range AF order. Due to the gauge interaction this gives rise to an insulating behavior of the resistivity in the same range of parameters where Fermi arcs exist. Since the current considered in this computation is the same considered in the computation made with the hole resonances, the spinon behavior of the resistivity is the dominating one, thus providing a solution to the puzzle of the FL arcs vs. NFL resistivity dichotomy. Furthermore, the spinon dominance explains the universality noticed in [3]. In fact, ref. [10] lets us normalize the resistivity as follows:

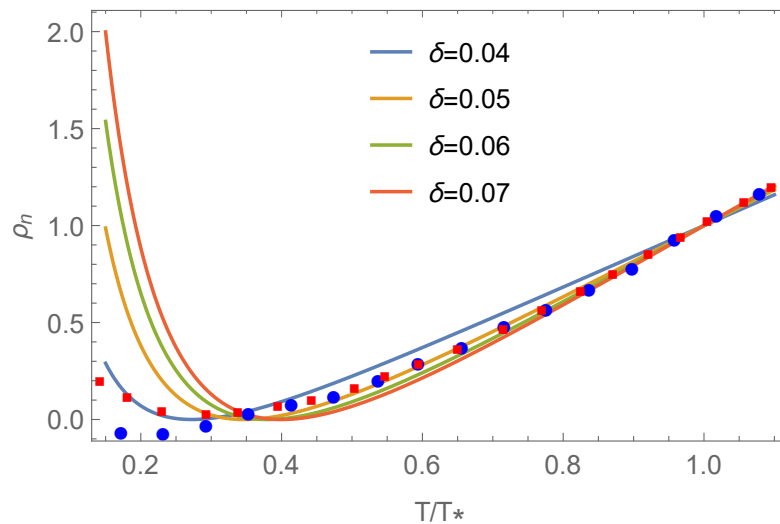$$\rho_n(T/T^*) = \frac{\rho(T/T^*) - \rho(T_{MIC}/T^*)}{\rho(1) - \rho(T_{MIC}/T^*)}. \tag{13}$$

Figure 4. Normalized in-plane resistivity ρ_n as a function of T/T^* calculated for various dopings. Red squares are data for ρ_n in LSCO taken from Ref. [2] for the non-superconducting samples at $\delta = 0.04, 0.05$; blue circles are data taken from the same reference for the superconducting samples at $\delta = 0.06, 0.07$ assuming $T_{MIC} = 0.3T^*$, as suggested by the data in the presence of a magnetic field or Zn-doping [41], in which an MIC also emerges for these dopings from the suppression of the superconductivity.

Then, as follows from Equation (12), neglecting the holon contribution ρ_n would be a universal function of the normalized temperature T/T^* and the characteristic temperature T^* itself is essentially determined by spinons. In the Ioffe–Larkin rule, a relative coefficient between the holon and the spinon contribution appears as a free parameter, independent of both T and δ, due to the use of a scale renormalization in the continuum limit adopted in the computation of the spinon contribution. An optimized coefficient, while adding a slight degree of non-universality, allows for a reasonably correct fit to experimental data, over a wide range of temperatures and dopings from T_{MIC} to T^*; see Figure 4.

Let us note as a marginal note [42] that the peculiar dependence on T of the "complex mass" $M_s = \sqrt{m_s^2 + ic\frac{\pi T}{\chi}}$ has produced for many decades of K the linear-in-T^2 behavior found in [43,44], without attributing it to the quasi-particle structure advocated there. A final remark: the inflection point in temperature of the in-plane resistivity identifying T^* in our formalism depends on a delicate cancellation between the doping dependence of the spinon gap m_s and the Fermi momenta of the holons, k_h^F : $T^* \sim m_s^2/k_F^h \sim \delta|\log\delta|/\delta$, and the result compares well with the experimental data. For this cancellation to occur it is crucial that $k_h^F \sim \delta$; it would not occur for the hole Fermi momenta $k^F \sim \sqrt{\delta}$.

5. Discussion

In this paper, we have presented evidence that the peculiar coexistence of Fermi arcs and metal–insulator crossover of in-plane resistivity in strongly underdoped cuprates can be attributed to the FL* nature of hole-doped cuprates. A qualitative agreement with experimental data is also exhibited for the hole-spectral weight and for the in-plane resistivity, including its universal property when suitably normalized. Following the strategy advocated here, a solution of the dichotomy of the spin susceptibility in the FL* approach was presented in [31]. Another phenomenon exhibiting coexistence of FL and non-FL features appears in the superconducting state of underdoped cuprates, where the superfluid density exhibit a non-BCS critical exponent and universality, whereas ARPES shows a standard BCS behavior near the nodes of the superconducting order parameter. Computations about this issue within the FL* framework are in progress, with positive preliminary results.

Appendix A

Since the self-energy of the hole is a key ingredient in the derivation of the Fermi arcs, in this appendix we sketch its derivation, referring the interested reader to [14,21,32] for further details.

Let us first consider the contribution due to the gauge interaction, Σ_g. Since the holon has a Fermi surface, to use our eikonal approximation involving first-quantization Feynman paths we first use a tomographic decomposition near the holon Fermi surface. This procedure is a kind of angle-dependent dimensional reduction, allowing us to rewrite the holon correlator as a sum of contributions from $1 + 1$ massless Dirac fields along each direction along the FS, following a strategy developed in [45–47]. The paths appearing for a direction are straight lines directed along the Fermi momenta of that direction (up to small transversal Gaussian fluctuations). We now multiply this path representation for the holon by that for the spinon, which is given by first-quantization Feynman(–Schwinger–Fradkin) paths of a massive particle [48]. The eikonal resummation is then obtained by first treating the slave-particle gauge field as an external field coupled to the holon paths,

using the Gorkov approximation, and to the spinon paths. One then integrates out the gauge field to obtain an interaction between these paths which is then treated in the eikonal approximation. In the scaling limit, only the magnetic components of the gauge field are relevant and the corresponding correlator at finite T is given by

$$\langle f_{ij}(x)f_{rs}(0)\rangle = (\delta_{ir}\delta_{js} - \delta_{is}\delta_{jr})\int \frac{dk^0}{2\pi}\int \frac{d\vec{k}}{(2\pi)^2}\frac{|\vec{k}|^2 e^{-ik^0 x^0 + i\vec{k}\cdot\vec{x}}}{i\frac{k^0}{|\vec{k}|}\kappa - \chi|\vec{k}|^2}\coth\left(\frac{k^0}{2T}\right). \tag{A1}$$

with $x = (x^0, \vec{x})$. In the presence of a probe in linear response theory given by an external field with frequency ω, the integration over k^0 should be cut off approximately by the maximum between T and ω. As an interpolation between the formulas with $\omega \gg$ and $\ll T$ we use the standard expression $\sqrt{(\pi T)^2 + \omega^2}$. The physics of Equation (A1) has as a typical scale the Reizer momentum $Q(T, \omega) = (\kappa\sqrt{(\pi T)^2 + \omega^2}/(\pi\chi))^{1/3}$. The leading effect of the gauge interaction on the spinon propagator can be described by a modification of the mass term in the exponent of $\exp im_s x^0$ given in the limit $x^0 \gg |\vec{x}|$ by

$$m_s x^0 \rightarrow \sqrt{m_s^2 - \frac{T}{\chi}g_1(|\vec{x}|Q)x^0 - \frac{T}{2\chi}Q^2 g_2(|\vec{x}|Q)\frac{(x^0)^2}{m_s^2}} \tag{A2}$$

where g_1 and g_2 are regular functions [14]. Finally, a Fourier transform is performed to obtain the retarded correlation function. In the evaluation of the spatial Fourier transform of the hole correlator, the shift (A2) generates a complex saddle point, α_{sp} for $\alpha \equiv |\vec{x}|Q$ and at the saddle point $g_1(\alpha_{sp}) = ic$, with $c \approx 1$, $g_2(\alpha_{sp}) \approx 0$. As a result, m_s is shifted to the complex mass M_s discussed in the text. The real part of the exponential $\exp[iM_s x^0]$ is monotonically decreasing in x^0; therefore, we estimate the x^0 integral by principal-part evaluation and scale renormalization to deal with the UV component. As a result, the frequency of the holon is shifted by M_s. The frequency- and temperature-independent part of $\Re M_s$ just renormalizes the holon chemical potential, shifting the FS of the holon to that of the hole. The imaginary part provides the gauge contribution to the self-energy Γ discussed in the text.

In the presence of the attraction generated by the AF spin vortices, the self-energy of the hole acquires another contribution, Σ_v. To estimate it, we calculate perturbatively at the leading order the effect of the phase of the holon pairs, ϕ, on the self-energy of the hole. Up to the square of the d-wave-order parameter, this is given by the convolution in momentum–frequency of the correlator of the fluctuations, $\exp i\phi$, with the previously derived hole correlator near the hole FS, where it is well defined. Due to the complication arising from the temperature dependence of Γ we proceed heuristically as follows: we estimate such a convolution in the Euclidean framework at 0 temperature and on the final result we perform the substitution $i\omega \rightarrow \omega + i\Gamma$. We first remark that the presence of the Maxwell gauge interaction due to the massive spinons suppresses the power correction $|\vec{x}|^{-1}$ in the Euclidean propagator of $\exp i\phi$ that would occur for a free massive field, leaving a purely exponential decay in x with inverse correlation length m_ϕ (see, e.g., [49]). In the Euclidean momentum $q = (q_0, \vec{q})$ space this can be reproduced by a propagator of the form $d[4\pi(q^2 + m_\phi^2)^{-1}]/dm_\phi$. If we denote by $E(\vec{q})$ the hole energy, the convolution that we need to evaluate is

$$\frac{d}{dm_\phi}\int\frac{d^3q}{(2\pi)^3}\frac{4\pi}{q^2 + m_\phi^2}\frac{1}{-i(q_0 - \omega) + E(\vec{q} - \vec{k})}. \tag{A3}$$

Since the dominant q are small we can expand E in (A3) linearly in q: let $\hat{k}$ denote the unit vector in the direction of $\vec{k}$, then

$$E(\vec{q} - \vec{k}) \approx -\vec{q}\cdot\hat{k} + E(\vec{k}). \tag{A4}$$

It is now convenient to fix a coordinate system for each direction $\hat{k}$ denoting by x the direction along $\hat{k}$ and by y the orthogonal one. One can then easily integrate out q_y, obtaining for the integral in (A3).

$$\frac{1}{2} \int \frac{dq_0 dq_x}{(2\pi)^2} \frac{4\pi}{\sqrt{q_0^2 + q_x^2 + m_\phi^2}} \frac{1}{-i(q_0 - \omega) + E(\vec{k}) - q_x}. \tag{A5}$$

Switching from (q_x, q_0) to the corresponding polar coordinates (r, θ) the above integral becomes

$$2\pi \int_0^\infty \frac{dr}{(2\pi)} \int_0^{2\pi} \frac{d\theta}{(2\pi)} \frac{r}{\sqrt{r^2 + m_\phi^2}} \frac{1}{i\omega + E(\vec{k}) - r \exp i\theta} = \int_0^\infty dr H(\sqrt{E(\vec{k})^2 + \omega^2} - r)$$

$$\frac{r}{\sqrt{r^2 + m_\phi^2}} \frac{r}{i\omega + E(\vec{k}) - r \exp i\theta} = \frac{\sqrt{E(\vec{k})^2 + \omega^2 + m_\phi^2} - m_\phi}{E(\vec{k}) + i\omega}, \tag{A6}$$

where H denotes the Heaviside step function. Differentiating by m_ϕ, then one obtains the self-energy Σ_v given in the text.

References

1. Sobota, J.A.; He, Y.; Shen, Z.-X.T. Angle-resolved photoemission studies of quantum materials. *Rev. Mod. Phys.* **2021**, *93*, 025006. [CrossRef]
2. Ando, Y.; Komiya, S.; Segawa, K.; Ono, S.; Kurita, Y. Electronic Phase Diagram of High-Tc Cuprate Superconductors from a Mapping of the In-Plane Resistivity Curvature. *Phys. Rev. Lett.* **2004**, *93*, 267001. [CrossRef] [PubMed]
3. Wuyts, B.; Moshchalkov, V.V.; Bruynseraede, Y. Resistivity and Hall effect of metallic oxygen-deficient YBa$_2$Cu$_3$O$_x$ films in the normal state. *Phys. Rev. B* **1996**, *53*, 9418–9432. [CrossRef]
4. Senthil, T.; Sachdev, S.; Vojta, M. Fractionalized Fermi Liquids. *Phys. Rev. Lett.* **2003**, *90*, 216403. [CrossRef] [PubMed]
5. Paramekanti, A.; Vishwanath, A. Extending Luttingers theorem to Z2 fractionalized phases of matter. *Phys. Rev. B* **1994**, *70*, 245118. [CrossRef]
6. Mei, J.-W.; Kawasaki, S.; Zheng, G.-Q.; Weng, Z.-Y.; Wen, X.G. Luttinger-volume violating Fermi liquid in the pseudogap phase of the cuprate superconductors. *Phys. Rev. B* **2012**, *85*, 134519. [CrossRef]
7. Sachdev, S. Emergent gauge fields and the high-temperature superconductors. *Philos. Trans. R. Soc. A* **2016**, *374*, 20150248. [CrossRef]
8. Seibold, G.; Arpaia, R.; Peng, Y.Y.; Fumagalli, R.; Braicovich, L.; Di Castro, C.; Grilli, M.; Ghiringhelli, G.C.; Caprara, S. Strange metal behaviour from charge density fluctuations in cuprates. *Commun. Phys.* **2021**, *4*, 7. [CrossRef]
9. Badoux, S.; Tabis, W.; Laliberté, F.; Grissonnanche, G.; Vignolle, B.; Vignolles, D.; Béard, J.; Bonn, D.A.; Hardy, W.N.; Liang, R.; et al. Change of carrier density at the pseudogap critical point of a cuprate superconductor. *Nature* **2016**, *351*, 210–214. [CrossRef]
10. Marchetti, P.A.; Bighin, G. Universality in Cuprates: A Gauge Approach. *J. Low Temp. Phys.* **2016**, *185*, 87–101. [CrossRef]
11. Baskaran, G.; Zou, Z.; Anderson, P.W. The resonating valence bond state and high-Tc superconductivity—A mean field theory. *Solid State Commun.* **1987**, *63*, 973–976. [CrossRef]
12. Kivelson, S.A.; Rokhsar, D.S.; Sethna, J.P. Topology of the resonating valence-bond state: Solitons and high-Tc superconductivity. *Phys. Rev. B* **1987**, *35*, 8865–8868. [CrossRef] [PubMed]
13. Marchetti, P.A.; Su, Z.-B.; Yu, L. U(1)XSU(2) Chern-Simons gauge theory of underdoped cuprate superconductors. *Phys. Rev. B* **1998**, *58*, 5808–5824. [CrossRef]
14. Marchetti, P.A.; De Leo, L.; Orso, G.; Su, Z.-B.; Yu, L. Spin-charge gauge approach to the pseudogap phase of high-Tc cuprates: Theory versus experiments. *Phys. Rev. B* **2004**, *69*, 024527. [CrossRef]
15. Marchetti, P.A.; Su, Z.-B.; Yu, L. Dimensional reduction of U(1) × SU(2) Chern-Simons bosonization: Application to the t-J model. *Nucl. Phys. B* **1996**, *482*, 731–757. [CrossRef]
16. Weng, Z.Y.; Sheng, D.N.; Chen, Y.-C.; Ting, C.S. Phase string effect in the t-J model: General theory. *Phys. Rev. B* **1997**, *55*, 3894–3906. [CrossRef]
17. Wilczek, F. *Fractional Statistics and Anyon Superconductivity*; World Scientific: Singapore, 1990.
18. Fröhlich, J.; Marchetti, P.A. Slave fermions, slave bosons, and semions from bosonization of the two-dimensional t-J model. *Phys. Rev. B* **1992**, *46*, 6535–6552. [CrossRef] [PubMed]
19. Hofstadter, D.R. Energy levels and wave functions of Bloch electrons in rational and irrational magnetic fields. *Phys. Rev. B* **1976**, *14*, 2239–2249. [CrossRef]

20. Rokhsar, D.S. Solitons in chiral-spin liquids. *Phys. Rev. Lett.* **1990**, *65*, 1506–1509. [CrossRef]

21. Marchetti, P.A. Fractional Statistics of Charge Carriers in the One- and Two-Dimensional t-J Model: A Hint for the Cuprates? *Condens. Matter.* **2020**, *5*, 12. [CrossRef]

22. Ye, F.; Marchetti, P.A.; Su, Z.-B.; Yu, L. Hall effect, edge states, and Haldane exclusion statistics in two-dimensional space. *Phys. Rev. B* **2015**, *92*, 235151. [CrossRef]

23. Marchetti, P.A.; Ye, F.; Su, Z.-B.; Yu, L. Charge carriers with fractional exclusion statistics in cuprates. *Phys. Rev. B* **2019**, *100*, 035103. [CrossRef]

24. Birgeneau, R.J. Antiferromagnetic spin correlations in insulating, metallic, and superconducting $La_{2-x}Sr_xCuO_4$. *Phys. Rev. B* **1988**, *38*, 6614–6623. [CrossRef]

25. Belinicher, V.I.; Chernyshev, A.L.; Dotsenko, A.V.; Sushkov, O.P. Hole-hole superconducting pairing in the *t-J* model induced by spin-wave exchange. *Phys. Rev. B* **1995**, *51*, 6076–6084. [CrossRef] [PubMed]

26. Marchetti, P.A.; Ye, F.; Su, Z.-B.; Yu, L. Hole pairing from attraction of opposite-chirality spin vortices: Non-BCS superconductivity in underdoped cuprates. *Phys. Rev. B* **2011**, *84*, 214525. [CrossRef]

27. Varma, C.M.; Littlewood, P.B.; Schmitt-Rink, S.; Abrahams, E.; Ruckenstein A.E. Phenomenology of the Normal State of Cu-0 High-Temperature Superconductors. *Phys. Rev. Lett.* **1989**, *63*, 1996–1999. [CrossRef]

28. Valla, T.; Fedorov, A.V.; Johnson, P.D.; Wells, B.O.; Hulbert, S.L.; Li, Q.; Gu, G.D.; Koshizuka, N. Evidence for Quantum Critical Behavior in the Optimally Doped Cuprate $Bi_2Sr_2CaCu_2O_{8+d}$. *Science* **1999**, *285*, 2110–2113. [CrossRef] [PubMed]

29. Bok, J.M.; Yun, J.H.; Choi, H.-Y.; Zhang, W.; Zhou, X.J.; Varma, C.M. Momentum dependence of the single-particle self-energy and fluctuation spectrum of slightly underdoped $Bi_2Sr_2CaCu_2O_{8+d}$ from high-resolution laser angle-resolved photoemission. *Phys. Rev. B* **2010**, *81*, 174516. [CrossRef]

30. Loktev, V.M.; Quick, R.M.; Sharapov, S.G. Phase fluctuations and pseudogap phenomena. *Phys. Rep.* **2001**, *349*, 1–123. [CrossRef]

31. Marchetti, P.A. FL* Interpretation of a Dichotomy in the Spin Susceptibility of the Cuprates. *Condens. Matter.* **2023**, *8*, 30. [CrossRef]

32. Marchetti, P.A.; Gambaccini, M. Gauge approach to the pseudogap phenomenology of the spectral weight in high Tc cuprates. *J. Phys. Condens. Matter.* **2012**, *24*, 475601. [CrossRef] [PubMed]

33. Kanigel, A.; Norman, M.R.; Randeria, M.M.; Chatterjee, U.; Souma, S.; Kaminski, A.; Fretwell, H.M.; Rosenkranz, S.; Shi, M.; Sato, T.; et al. Evolution of the pseudogap fromFermi arcs to the nodal liquid. *Nat. Phys.* **2006**, *2*, 447–451. [CrossRef]

34. Kondo, T.; Malaeb, W.; Ishida, Y.; Sasagawa, T.; Sakamoto, H.; Takeuchi, T.; Tohyama, T.; Shin, S. Point nodes persisting far beyond Tc in Bi2212. *Nat. Commun.* **2015**, *6*, 7699. [CrossRef] [PubMed]

35. Yang, K.-Y.; Rice, T.M.; Zhang, F.-C. Phenomenological theory of the pseudogap state. *Phys. Rev. B* **2006**, *73*, 174501. [CrossRef]

36. Yoshida, T.; Zhou, X.J.; Lu, D.H.; Komiya, S.; Ando, Y.; Eisaki, H.; Kakeshita, T.; Uchida, S.; Hussain, Z.; Shen, Z.-X.; et al. Low-energy electronic structure of the high-Tc cuprates $La_{2-x}Sr_xCuO_4$ studied by angle-resolved photoemission spectroscopy. *J. Phys. Condens. Matter.* **2007**, *19*, 125209. [CrossRef]

37. Rullier-Albenque, F.; Alloul, H.; Balakirev, F.; Proust, C. Disorder, metal-insulator crossover and phase diagram in high-Tc cuprates. *Euro Phys. Lett.* **2008**, *81*, 37008. [CrossRef]

38. Ioffe, L.B.; Larkin, A. Gapless fermions and gauge fields in dielectrics. *Phys. Rev. B* **1989**, *39*, 8988–8999. [CrossRef] [PubMed]

39. Lee, P.A.; Nagaosa, N. Gauge theory of the normal state of high-Tc, superconductors. *Phys. Rev. B* **1992**, *46*, 5621–5639. [CrossRef] [PubMed]

40. Ioffe, L.B.; Wiegmann, P.B. Linear Temperature Dependence of Resistivity as Evidence of Gauge Interaction. *Phys. Rev. Lett.* **1990**, *65*, 653–656. [CrossRef]

41. Komiya, S.; Ando, Y. Electron localization in $La_{2-x}Sr_xCuO_4$ and the role of stripes. *Phys. Rev. B* **2004**, *70*, 060503. [CrossRef]

42. Marchetti, P.A.; Su, Z.-B.; Yu, L. Transport properties of HTS cuprates via spin-charge gauge approach. *Phys. C* **2007**, *460–462*, 1081–1083. [CrossRef]

43. Ando, Y.; Kurita, Y.; Komiya, S.; Ono, S.; Segawa, K. Evolution of the Hall Coefficient and the Peculiar Electronic Structure of the Cuprate Superconductors. *Phys. Rev. Lett.* **2004**, *92*, 197001. [CrossRef] [PubMed]

44. Barišić, N.; Chan, M.K.; Li, Y.; Yu, G.; Zhao, X.; Dressel, M.; Smontara, A.; Greven, M. Universal sheet resistance and revised phase diagram of the cuprate high-temperature superconductors. *Proc. Natl. Acad. Sci. USA* **2013**, *110*, 12235–12240. [CrossRef] [PubMed]

45. Benfatto, G.; Gallavotti, G. Perturbation Theory of the Fermi Surface in a Quantum Liquid. A General Quasiparticle Formalism and One-Dimensional Systems. *J. Stat. Phys.* **1990**, *59*, 541. [CrossRef]

46. Chen, T.; Fröhlich, J.; Seifert, M. Renormalization group methods: Landau-Fermi liquid and BCS superconductor. In Proceedings of the Les Houches Summer School, Session 62: Fluctuating Geometries in Statistical Mechanics and Field Theory, Les Houches, France, 2 August–9 September 1994.

47. Shankar, R. Renormalization-group approach to interacting fermions. *Rev. Mod. Phys.* **1994**, *66*, 129. [CrossRef]

48. Fried, H.M. *Green's Functions and Ordered Exponentials*; Cambridge University Press: Cambridge, UK, 2002.
49. Bricmont, J.; Fröhlich, J. Statistical mechanical methods in particle structure analysis of lattice field theories: (I). General theory. *Nucl. Phys.* **1985**, *251*, 517–552. [CrossRef]